

Short Communication

Photoelectrochemical Reduction of Carbon Dioxide to Ethanol at Cu₂O Foam Cathode

Jiongliang Yuan^{1,*}, Bin Xiao², Cunjiang Hao³

¹ Department of Environmental Science and Engineering, Beijing University of Chemical Technology, Beijing 100029, P. R. China

² College of Chemical Engineering, Beijing University of Chemical Technology, Beijing 100029, P. R. China

³ Department of Experimental Teaching, Tianjin University of Traditional Chinese Medicine, and Tianjin Key Laboratory of Chemistry and Analysis of Chinese Materia Medica, Tianjin 300193, P. R. China

*E-mail: yuanjiongliang@163.com

Received: 8 May 2017 / Accepted: 3 July 2017 / Published: 13 August 2017

Direct reduction of CO₂ to ethanol with a high rate at a low overpotential is quite difficult. In this study, the Cu₂O foam electrode with three-dimensional coaxial network structure is fabricated by electrodeposition of Cu₂O coatings on copper foam substrate. It shows unprecedented photoelectrocatalytic performance on the reduction of CO₂ to ethanol. The formation rate of ethanol as high as 71.67 μmol cm⁻² h⁻¹ is obtained at the overpotential as low as 131 mV within 1.5 h.

Keywords: Carbon dioxide, Ethanol, Photoelectrochemical reduction, Cuprous oxide, Foam electrode.

1. INTRODUCTION

The rapid increase of CO₂ gas in the atmosphere causes serious global warming. Some technologies of CO₂ capture, sequestration and conversion have been developed, among which the technology of converting CO₂ into useful chemicals is the most promising [1,2]. Converting CO₂ to ethanol will promote closed cycle of CO₂, and ethanol can be used as fuels and chemicals.

CO₂ can be reduced to ethanol by electrochemical method, and the catalysts such as metallic Cu, Cu oxides have been developed [3-7]. At metallic Cu electrode, CO₂ is reduced to ethanol at extremely high overpotential (>0.9 V), and the faradaic efficiency of ethanol formation is less than 10% [4,5]. At Cu₂O electrode, CO₂ is reduced to ethanol, formic acid and methanol, among which ethanol is the major product [6]. However, Cu₂O electrode is unstable, and can be reduced to metallic

Cu within 30 min; the faradaic efficiency of ethanol formation decreases from 96.2% at 5 min to 38.5% at 25 min [6]. CuO/carbon paper electrodes have been fabricated for CO₂ reduction, and the product ethanol is obtained [7]. Nevertheless, CuO electrode is also unstable [7]. At Cu₂O and CuO electrodes, the overpotential of the reduction of CO₂ to ethanol is extremely high (>1.0 V), and the high overpotential promotes the reduction of Cu₂O and CuO to metallic Cu, which causes the poor stability of Cu₂O and CuO electrodes [7]. In our previous study, pyridine cocatalyst can decrease the overpotential of CO₂ reduction via the formation of the intermediate, C₅H₅N-H⁺...O=C=O [8].

Due to large surface area, well-defined pore size, good hydrodynamic characteristics and high conductivity, copper foam substrates are better supports for catalysts than conventional planar supports. It is expected to improve the catalytic performance of Cu₂O for CO₂ reduction by loading Cu₂O catalysts on copper foam support. In this study, using the Cu₂O foam electrode as the photocathode and pyridine as the cocatalyst, CO₂ is reduced photoelectrochemically to ethanol with a high rate at a low overpotential.

2. EXPERIMENTAL

2.1 Fabrication of Cu₂O foam electrodes

Cu₂O foam electrodes were fabricated by electrodeposition of Cu₂O coatings on copper foam substrates. A copper foam substrate (the working area is 2 cm² and the thickness is 0.5 mm), platinum foil and saturated calomel electrode (SCE) were used as the working electrode, the counter electrode and the reference electrode, respectively. The electrolytic solution (50 mL) containing 0.4 mM CuSO₄ and 3 M lactic acid was adjusted to pH 10 by adding concentrated NaOH aqueous solution [9,10]. The electrodeposition was employed for 20 min at -0.60 V (vs. SCE) and 60 °C.

The morphology of Cu₂O foam electrode was determined by a field emission scanning electron microscopy (FESEM, S-4700, Hitachi, Japan). The crystal structure of Cu₂O coatings was determined by X-ray diffractometry (XRD, Bruker D8 Advance, Germany), and the crystal grain size was then calculated from X-ray line broadening using the Scherrer's equation. The UV-Vis spectrum of Cu₂O foam electrode was measured with UV-vis-NIR spectrophotometer (UV-3600, Shimadzu, Japan).

2.2 Photoelectrochemical reduction of CO₂

The solar-driven photoelectrochemical reduction of CO₂ was performed in 0.1 M acetate buffer solution (50 mL) containing 30 mM pyridine. A conventional three-electrode cell was used with Cu₂O foam electrode (working area is 2 cm²) as the working electrode, the graphite sheet as the counter electrode and SCE as the reference electrode. The irradiation intensity on the working electrode was calibrated to be 100 mW cm⁻². Before the reduction experiment, the electrolyte solution was bubbled with CO₂ gas (99.99%) for 30 min. CO₂ gas was constantly introduced into the electrolyte solution at a flow rate of 60 mL min⁻¹ during the whole experiment. Liquid product analysis was accomplished using gas chromatography-mass spectroscopy (GC-MS, Trace 1300-ISQ, ThermoFisher Scientific,

USA), and ethanol concentration was measured by a gas chromatography (GC 2014C, Shimadzu, Japan) with a DB-Wax (30 m×0.53 mm×3.00 μm, Agilent Technologies). The injector temperature was held at 200 °C, the oven temperature rose from 50 to 200 °C at a rate of 5 °C min⁻¹, and the detector temperature was kept at 230 °C. Five runs were done for one experiment.

The linear scanning voltammetric measurement of the Cu₂O foam electrode was conducted in the above setup, and the scanning potential was set from 0 to -1.000 V (vs. SCE) at 5 mV s⁻¹. The current density was determined on the geometric area of the foam electrode (2 cm²).

3. RESULTS AND DISCUSSION

3.1 Fabrication and characterization of Cu₂O foam electrodes

The FESEM images of Cu₂O foam electrode are shown in Fig. 1. The Cu₂O foam electrode has well-developed porous structure, and the pore size is about 400 μm, and it exhibits three-dimensional coaxial network structure of outer Cu₂O tube and inner Cu wire, which facilitates the light-driven charges in Cu₂O semiconductor to transfer rapidly along Cu wire to the external circuit, thus promoting the separation of light-driven charges. It is observed that Cu₂O coatings on copper foam substrate have the thickness of about 2 μm, and the surface of Cu₂O coatings exhibits truncated pyramid geometry, similar to Cu₂O thin films electrodeposited on stainless steel substrates [9].

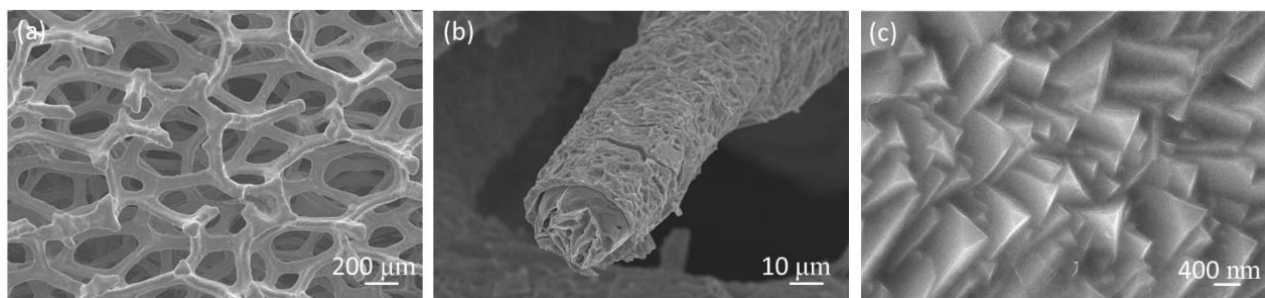


Figure 1. FESEM images of the Cu₂O foam electrode. (a) full view, (b) cross section view, (c) enlarged surface.

The XRD pattern of the Cu₂O foam electrode is presented in Fig. 2. The peaks at 43.4, 50.5 and 74.1° can be indexed to Cu (111), (200) and (222) facets. The peaks at 29.8, 37.4 42.6 and 61.8° can be indexed to cuprite Cu₂O (110), (111), (200) and (220) facets, and a very strong peak at 37.4° indicates that Cu₂O crystal grows preferentially along (111) facet. It has been reported that the preferential growth facet of Cu₂O is dependent on pH of electrodeposition solution, and it is (111) facet at pH>9 [11]. The grain size of Cu₂O, estimated from XRD pattern, is about 26.5 nm.

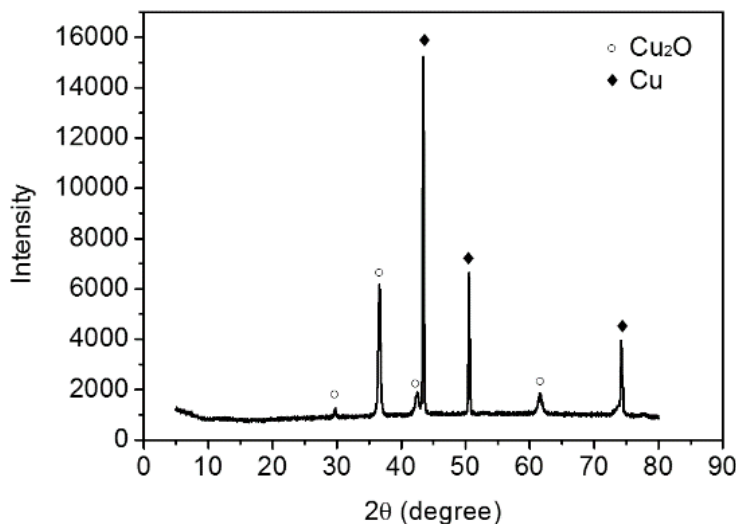


Figure 2. XRD of the Cu_2O foam electrode.

Fig. 3 shows the UV-vis spectrum of the Cu_2O foam electrode. The Cu_2O foam electrode exhibits strong absorbance in the visible light range, especially in 400-550 nm range. The bandgap is estimated to be 1.95 eV by Tauc equation.

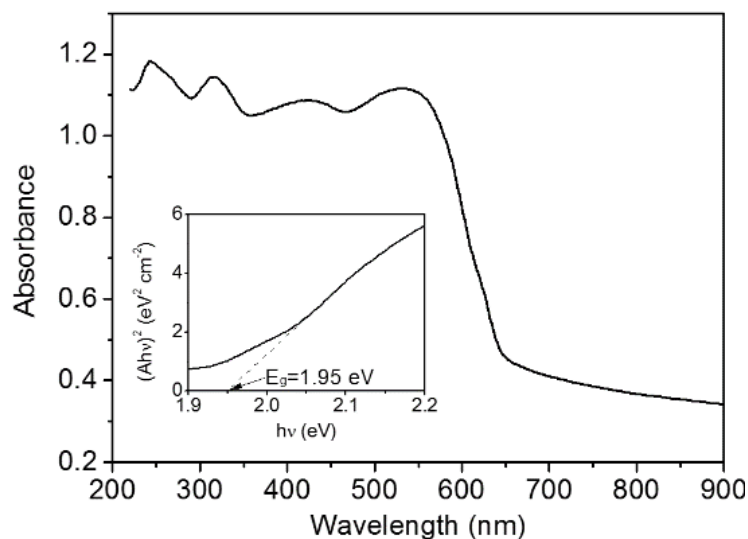


Figure 3. UV-vis spectrum of the Cu_2O foam electrode and the bandgap value (inset).

3.2 Photoelectrochemical reduction of CO_2 at Cu_2O foam cathodes

Linear scanning voltammetric curves of the Cu_2O foam electrode in dark and under illumination in 0.1 M acetate buffer solution containing saturated CO_2 and 30 mM pyridine are compared in Fig. 4. In contrast to the voltammetric behavior in dark, a dramatic increase in peak current density at -0.60 V (vs. SCE) is observed under illumination, indicating that the reduction of CO_2 becomes significant.

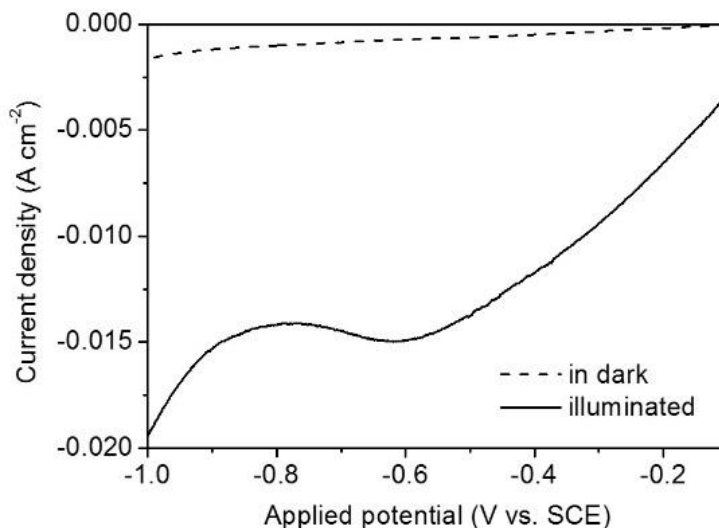


Figure 4. Linear scanning voltammetric curve of the Cu₂O foam electrode.

In the liquid product of photoelectrocatalytic reduction of CO₂, only ethanol as the reaction product is detected by GC-MS. When the photoelectrochemical reaction is employed with the introduction of nitrogen gas rather than CO₂ gas, no ethanol is detected in the reaction product, indicating that ethanol is not derived from acetic acid, sodium acetate or pyridine, but from CO₂.

Ethanol concentration at various applied potential is shown in Table 1. It reveals that the applied potential has a significant influence on ethanol concentration. Ethanol concentration increases with increasing potential from -0.55 to -0.60 V (vs. SCE), and it achieves the optimum at -0.60 V; then it decreases with increasing potential from -0.60 to -0.70 V. The relationship between applied potential and ethanol concentration is similar to that between applied potential and current density as shown in Fig. 4. At -0.60 V, it adds up to 4.3 mM in 1.5 h; namely, the average formation rate of ethanol is 71.67 $\mu\text{mol cm}^{-2} \text{h}^{-1}$ within 1.5 h, which is much higher than that in previous studies [6,7,12]. The high formation rate of ethanol can be attributed to high specific surface area which promotes the full contact of the catalytic active centers with the reactants in photoelectrochemical reduction of CO₂.

Table 1. Ethanol concentration at various applied potential.

Applied potential (V vs. SCE)	Ethanol concentration (mM)
-0.55	2.19
-0.60	4.28
-0.65	1.82
-0.70	1.26

Yadav et al. has proposed that, at above 1.5 V, Cu₂O cathode with the preferential (200) facet can reduce CO₂ to ethanol in KHCO₃ solution [6]. The extremely high overpotential is resulted from the high electrode potential of CO₂/CO₂⁻ (-1.90 V vs. normal hydrogen electrode) [6]. In this study,

pyridine cocatalyst decreases the overpotential of CO₂ reduction, and the highest formation rate of ethanol is obtained at -0.60 V (vs. SCE), that is, at the overpotential of 131 mV.

Since the reduction potential of CO₂ decreases in this study, the reduction of Cu₂O becomes less significant, and the stability of Cu₂O foam electrodes is enhanced. However, the activity of Cu₂O foam electrodes in this study decreases after 1.5 h. Therefore, the stability of Cu₂O foam electrodes needs to improve further.

At the same Cu₂O foam electrode, methanol is obtained in KHCO₃ solution in our previous study [10]; in contrast, ethanol is produced in acetate buffer solution containing pyridine in the present study. It indicates that the electrolytic solution has a significant effect on the product species.

The possible reaction intermediates, methanol, acetaldehyde and formic acid are introduced in the electrolyte solution to replace CO₂ as the reactant, respectively. It is observed that ethanol occurs in the electrolyte solution containing methanol, and ethanol concentration increases with the reaction time, accompanied by the decrease of methanol concentration. However, no ethanol occurs in the electrolyte solution containing acetaldehyde or formic acid. It indicates that methanol might be the intermediate in the reduction of CO₂ to ethanol. The mechanism needs further investigation.

4. CONCLUSIONS

The Cu₂O foam electrode with three-dimensional network structure has been fabricated by electrodeposition of Cu₂O coatings on copper foam substrate, and it has the coaxial structure of Cu₂O tube and Cu wire. The Cu₂O foam electrode exhibits strong absorbance in visible light range, and its bandgap is estimated to be 1.95 eV. At the Cu₂O foam photocathode, solar driven photoelectrochemical reduction of CO₂ to ethanol occurs with a high rate at a low overpotential. The formation rate of ethanol as high as 71.67 μmol cm⁻² h⁻¹ is obtained at the overpotential as low as 131 mV within 1.5 h. Methanol might be the intermediate in the reduction reaction of CO₂ to ethanol.

ACKNOWLEDGEMENTS

The project is funded by Special Found for Beijing Common Construction Project (Grant No. jwgj201707) and National Natural Science Foundation of China (Grant No. 21676010).

References

1. M. E. Boot-Handford, J. C. Abanades, E. J. Anthony, M. J. Blunt, S. Brandani, N. Mac Dowell, J. R. Fernandez, M. C. Ferrari, R. Gross, J. P. Hallet, R. S. Haszeldine, P. Heptonstall, A. Lyngfelt, Z. Makuch, E. Mangano, R. T. J. Porter, M. Pourkashanian, G. T. Rochelle, N. Shah, J. G. Yao and P. S. Fenell, *Energy Environ. Sci.*, 7 (2014) 130.
2. J. Albo, Alfonso Sáez, J. Solla-Gullón, V. Montiel and A. Iribien, *Appl. Catal. B: Env.*, 176–177 (2013) 709.
3. J. Qiao, Y. Liu, F. Hong and J. Zhang, *Chem. Soc. Rev.*, 43 (2014) 631.
4. K. P. Kuhl, E. R. Cave, D. N. Abram and T. F. Jaramillo, *Energy Environ. Sci.* 5 (2012) 7050.
5. M. Gattrell, N. Gupta and A. Co, *J. Electroanal. Chem.*, 594 (2006) 1.

6. V. S. K. Yadav and M. K. Purkait, *Energy Fuels*, 29 (2015) 6670.
7. D. Chi, H. Yang, Y. Du, T. Lv, G. Sui, H. Wang and J. Lu, *RSC Adv.*, 4 (2014) 37329.
8. J. Yuan, L. Zheng and C. Hao, *RSC Adv.*, 4 (2014) 39435.
9. M. Le, M. Ren, Z. Zhang, P. T. Sprunger, R. L. Kurtz and J. C. Flake, *J. Electrochem. Soc.*, 158 (2016) E45.
10. J. Yuan, X. Wang, C. Gu, J. Sun, W. Ding, J. Wei, X. Zuo and C. Hao, *RSC Adv.*, 7 (2017) 24933.
11. S. S. Jeong, A. Mittiga and E. Salza, *Electrochim. Acta*, 53 (2008) 2226.
12. J. Yuan, X. Wang and F. Zhang, *J. Electrochem. Soc.*, 163 (2016) E305.

© 2017 The Authors. Published by ESG (www.electrochemsci.org). This article is an open access article distributed under the terms and conditions of the Creative Commons Attribution license (<http://creativecommons.org/licenses/by/4.0/>).